Theoretical Ecology (2018) 11:453–463
https://doi.org/10.1007/s12080-018-0378-z

ORIGINAL PAPER

Accounting for activity respiration results in realistic trophic transfer efficiencies in allometric trophic network (ATN) models

Nadja J. Kath [1] · Alice Boit [1] · Christian Guill [1] · Ursula Gaedke [1]

Received: 4 August 2017 / Accepted: 3 May 2018 / Published online: 19 May 2018

Abstract
Allometric trophic network (ATN) models offer high flexibility and scalability while minimizing the number of parameters and have been successfully applied to investigate complex food web dynamics and their influence on food web diversity and stability. However, the realism of ATN model energetics has never been assessed in detail, despite their critical influence on dynamic biomass and production patterns. Here, we compare the energetics of the currently established original ATN model, considering only biomass-dependent basal respiration, to an extended ATN model version, considering both basal and assimilation-dependent activity respiration. The latter is crucial in particular for unicellular and invertebrate organisms which dominate the metabolism of pelagic and soil food webs. Based on metabolic scaling laws, we show that the extended ATN version reflects the energy transfer through a chain of four trophic levels of unicellular and invertebrate organisms more realistically than the original ATN version. Depending on the strength of top-down control, the original ATN model yields trophic transfer efficiencies up to 71% at either the third or the fourth trophic level, which considerably exceeds any realistic values. In contrast, the extended ATN version yields realistic trophic transfer efficiencies ≤ 30% at all trophic levels, in accordance with both physiological considerations and empirical evidence from pelagic systems. Our results imply that accounting for activity respiration is essential for consistently implementing the metabolic theory of ecology in ATN models and for improving their quantitative predictions, which makes them more powerful tools for investigating the dynamics of complex natural communities.

Keywords Food web · Trophic transfer efficiency · Allometric trophic network model · Allometry · Energy transfer · Activity respiration

Introduction

The metabolic theory of ecology relates biological rates to body size and serves to predict metabolic activity from the individual to the community level (Brown et al. 2004). Allometrically scaled trophic network (ATN) models implement this theory in a food web context by linking consumers to their resources in food webs. Yodzis and Innes (1992) parameterized the first ATN model which is the theoretical basis of a fruitful series of ATN modeling studies for ecological theory building, e.g., contributing to the diversity-stability debate (Benoît and Rochet 2004; Brose et al. 2006; Heckmann et al. 2012), coexistence theory (Brose 2008), hypotheses on biodiversity-ecosystem functioning (Schneider et al. 2016), and for investigating biodiversity loss (Berlow et al. 2009; Schneider et al. 2012). The main advantage of ATN models is their scalability from small modules to large and complex food webs in a widely applicable approach with only few assumptions.

The ATN approach builds upon the fact that material ingested by a consumer is either excreted or allocated to respiration or production (Fig. 1). The assimilation efficiency differs for carnivores and herbivores because of the respective food's quality and stoichiometry. Regarding losses to respiration, all previous studies with ATN models except for Boit et al. (2012) and Kuparinen et al. (2016) considered

✉ Nadja J. Kath
nkath@uni-potsdam.de

[1] Institut für Biochemie und Biologie, Universität Potsdam, Maulbeerallee 2, 14469 Potsdam, Germany

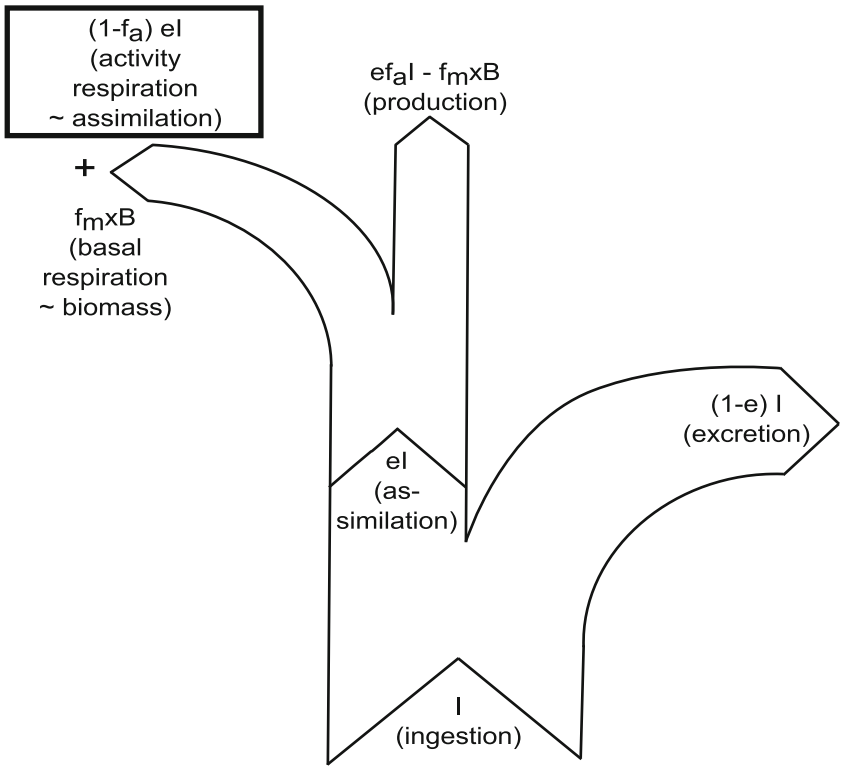

Fig. 1 The carbon (surrogate for energy) flow scheme implemented in the ATN model approach. The original version by Yodzis and Innes (1992) does not separate activity from basal respiration, but assumes that all respiration is proportional to biomass. The missing part of activity respiration proportional to assimilation (box) is added to the original ATN model in this study. Model parameters are e assimilation efficiency, f_a factor accounting for activity respiration, f_m factor accounting for basal respiration, x metabolic rate, B biomass, and I ingestion (for details see Table 1 and "Methods")

only respiration proportional to biomass, here called basal respiration, whereas respiratory losses due to activity, hereafter called activity respiration, were not specifically accounted for. This approximation may apply to homoiothermic mammals and birds with high maintenance costs. However, it appears less suitable for modeling pelagic and soil food webs, which mostly consist of unicellular and invertebrate organisms with low basal respiration, but high activity respiration, which is proportional to food uptake (Anderson 1992). The study by Boit et al. (2012) on the seasonal plankton succession in Lake Constance already indicated that the ATN model successfully reproduced general community patterns only if the important physiological process of activity respiration was accounted for. In contrast, the original ATN model considerably overestimated heterotrophic production if activity respiration was ignored (Boit et al. 2012). Kuparinen et al. (2016) used the ATN model as extended by Boit et al. (2012) to successfully model the effects of fishing on a food web and the fish life-history traits. These two studies called for the in-depth evaluation of ATN model energetics which we present in this work. To differentiate between the two model versions, we employ the terms "original" (Yodzis and Innes 1992) and "extended" ATN model (Boit et al. 2012).

To quantify and evaluate model energetics, we determine the trophic transfer efficiency (TTE) between four ascending trophic levels (autotrophs, herbivores, carnivores, and top predators) for both the original and the extended ATN versions. We find that only by accounting for activity respiration, the ATN model achieves realistic TTE towards the higher trophic levels. To explain this model behavior, we additionally compared biomasses, respiration, and production of both model versions for different levels of top predator mortality. The latter elucidates the influence of top-down vs. bottom-up control on the TTE and the formation of trophic cascades. We discuss our findings in the context of previous modeling studies and observations from pelagic systems to promote the inclusion of activity respiration in future ATN models. Achieving more realistic energetics and improving quantitative predictions will make ATN models more powerful tools to investigate complex natural food webs in order to better serve their purpose in ecological theory building.

Methods

Allometric trophic network (ATN) models represent consumer-resource relationships based on allometric scaling of key physiological rates (e.g., ingestion) with individual body mass, which achieves minimum data necessity for model parameterization (Yodzis and Innes 1992). Ingested carbon serves as surrogate for energy and is allocated to either excretion, respiration, or production (Fig. 1, Begon et al. 2006). The original ATN model formulation does not differentiate between basal respiration proportional to the biomass, and

activity respiration proportional to the amount of assimilated food (Fig. 1).

General ATN model equations and parameters

We applied the ATN model equations to a linear chain of four trophic levels from autotrophs (A) and herbivores (H) to carnivores (C) and top predators (T). In order to facilitate comparability between studies, our notation and parameterization closely follow that of previous ATN modeling studies (Brose et al. 2006; Boit et al. 2012). Growth of the autotrophs is modeled by a logistic function (Eq. 1), and consumption by all consumers is described by a Holling type II functional response (Eqs. 1–4, Holling 1959). Together, the rates of change of the biomasses B_i (i = A, H, C, T) at the four trophic levels are given by the following ordinary differential equations:

$$\frac{dB_A}{dt} = rB_A\left(1-\frac{B_A}{K}\right)-yx_H\frac{B_A}{B_0+B_A}B_H \quad (1)$$

$$\frac{dB_H}{dt} = f_a e_h y x_H \frac{B_A}{B_0+B_A}B_H - yx_C\frac{B_H}{B_0+B_H}B_C - f_m x_H B_H \quad (2)$$

$$\frac{dB_C}{dt} = f_a e_c y x_C \frac{B_H}{B_0+B_H}B_C - yx_T\frac{B_C}{B_0+B_C}B_T - f_m x_C B_C \quad (3)$$

$$\frac{dB_T}{dt} = f_a e_c y x_T \frac{B_C}{B_0+B_C}B_T - f_m x_T B_T - dB_T{}^2. \quad (4)$$

The maximum growth rate of the autotrophs is described by r and their carrying capacity by K. The functional responses for consumption are expressed by the metabolic rate of the respective consumer, x_H, x_C, x_T, the maximum ingestion rate y normalized by the respective metabolic rate, and the half-saturation constant B_0. The assimilation efficiency for herbivores is denoted as e_h, the one for carnivorous predators as e_c, the fraction of assimilated carbon not respired is defined by f_a, i.e., (1-f_a) is the fraction of carbon lost by activity respiration, and the fraction of maintenance respiration linked to biomass is f_m. The metabolic rates x_i scale allometrically with body mass m_i with an allometric exponent of − 0.25 (Yodzis and Innes 1992). The autotrophs' body mass is set to 1 and the consumer-resource body-mass ratio is 1000 for all trophic levels. The standard values of all parameters are given in Table 1. The death rate constant of the top predator is given by d (Eq. 4, Table 1), and it was varied between 0 and 0.05 in steps of 0.0001. The term dB_T represents the top predator's per capita death rate. The case $d = 0$ represents an extreme case as it leads to a massive accumulation of top predator biomass which in nature would attract pathogens, parasites, or another carnivore, which all induce mortality.

Calculation of central rates

All central rates, i.e., ingestion, excretion, basal and activity respiration, and production have the same dimension mass × volume^{-1} × time^{-1}. The total ingestion rate I_i of the consumer species on trophic level i with biomass B_i is given by

$$I_i = yx_i\frac{B_{i-1}}{B_0+B_{i-1}}B_i. \quad (5)$$

Multiplied with the assimilation constant e_i and the activity respiration factor f_a, the term I_i constitutes the first term in Eqs. 2–4. The total excretion rate E_i of trophic level i is proportional to its ingestion rate and is given by

$$E_i = (1-e_i)I_i = (1-e_i)yx_i\frac{B_{i-1}}{B_0+B_{i-1}}B_i. \quad (6)$$

The assimilation efficiency e_i describes the fraction of the ingested material that is assimilated and not lost by excretion. It is higher for carnivores than for herbivores

Table 1 Parameter values. If the original and extended ATN versions are differently parameterized, their values are labeled with $^{orig.}$ and $^{ext.}$, respectively. Dimensionless units are labeled as [−]

Parameter name	Abbreviation	Value [dimension]	Literature
Mass-specific maximum growth rate of the autotrophs	r	1 $[\frac{1}{time}]$	(Brose et al. 2006)
Carrying capacity	K	1 $[\frac{mass}{volume}]$	(Brose et al. 2006)
Metabolic rate	x_i	0.314 $mass_i^{-0.25}$ $[\frac{1}{time}]$	(Brose et al. 2006)
Maximum ingestion rate relative to metabolic rate	y	8 [−]	(Brose et al. 2006)
Half-saturation constant	B_0	0.5 $[\frac{mass}{volume}]$	(Brose et al. 2006)
Fraction of assimilated carbon used for production	f_a	1^{orig} /0.4^{ext} [−]	(Boit et al. 2012)
Factor for maintenance respiration	f_m	1^{orig} /0.1^{ext} [−]	Boit et al. 2012)
Assimilation efficiency for herbivorous species	e_h	0.45 [−]	(Yodzis and Innes 1992)
Assimilation efficiency for carnivorous species	e_c	0.85 [−]	(Yodzis and Innes 1992)
Death rate constant of top predator	d	[0, 0.05] $[\frac{volume}{time\ mass}]$	Varied in this study

(Table 1) since the former consume high-quality food of similar biochemical composition as themselves, whereas plants often contain nutrient-poor material which is hard to digest.

Basal respiration is the energy lost due to maintenance processes. It is analog to the basal metabolic rate defined for homoiotherms (Gessaman 1973) as measured in the thermoneutral zone where homoiotherms have very low costs for thermoregulation and are most similar to ectotherms in this regard. Basal respiration $R_{b,i}$ is defined as

$$R_{b,i} = f_m x_i B_i \tag{7}$$

and is therefore proportional to the standing stock biomass. Activity respiration is the energy spent for processes related to the production of new biomass (including locomotion, foraging, food handling and digestion, ontogenetic processes, and reproduction). We call f_a the fraction of energy not lost due to activity processes. Following Boit et al. (2012), the activity respiration $R_{a,i}$ is calculated as

$$R_{a,i} = (1-f_a)\, e_i\, I_i = (1-f_a) e_i y x_i \frac{B_{i-1}}{B_0 + B_{i-1}} B_i. \tag{8}$$

This part is neglected in the original ATN model, i.e. $f_a = 1$.

The production summarizes all processes that lead to creation of new biomass (somatic and reproductive growth). On average, the production at trophic level i compensates for losses by predation, i.e., the ingestion by trophic level $i+1$. If we neglect non-grazing mortality, which typically plays a minor role in pelagic systems (Gaedke et al. 2002), the production P_i can either be calculated as ingestion of the next higher trophic level I_{i+1} or as ingestion at trophic level i minus excretion E_i and total respiration $R_i = R_{a,i} + R_{b,i}$,

$$P_i = I_{i+1} = I_i - E_i - R_{a,i} - R_{b,i}. \tag{9}$$

For the top predator, the ingestion by a higher trophic level is replaced by its death rate dB_T^2 (Eq. 4). These different ways to calculate the production (Eq. 9) enable us to infer the trophic transfer efficiencies.

Trophic transfer efficiency

The trophic transfer efficiency (TTE) is defined as the ratio of the production of two adjacent trophic levels and is therefore dimensionless. It is used to quantify the fraction of energy passed on to the next trophic level. To calculate the maximum TTE, it is crucial to remember that ingested carbon can only be excreted, respired, or invested into new production (Fig. 1). When one of the first two rates increases, the production decreases. Following Yodzis and Innes (1992), carnivores are assumed to have an assimilation efficiency of 85% and herbivores of 45% (Table 1). From physiological considerations based on a comprehensive data set across different taxonomic groups (Humphreys 1979; Hendriks 1999), it can be estimated that at most half of the assimilated carbon can be allocated to production (Fig. 1), which yields an upper limit to the maximum feasible TTE_i between trophic level i and $i+1$:

$$\text{Maximum feasible } \mathrm{TTE}_{i\to i+1} \le 0.5\, \frac{e_{i+1}\, I_{i+1}}{P_i}. \tag{10}$$

This results in a maximum feasible TTE of at most 42.5% of the ingested carbon for carnivores and of 22.5% for herbivores (cf. Table 2). Note that this is a very conservative estimation. Most taxa have considerably higher respiratory losses and thus lower production to assimilation ratios, resulting in a lower maximum feasible TTE.

One way to calculate the TTE to the next trophic level in the model is

$$TTE_{i\to i+1} = \frac{P_{i+1}}{P_i} = \frac{e_{i+1} I_{i+1} - \left(R_{a,i+1} + R_{b,i+1}\right)}{I_{i+1}} = \frac{f_a e_{i+1} y \frac{B_i}{B_h + B_i} - f_m}{y \frac{B_i}{B_h + B_i}}. \tag{11}$$

This expression has an upper limit that is reached for unlimited food supply $B_i \to \infty$. For this limit, the rightmost part of Eq. 11 can be simplified to

$$TTE_{i\to i+1} < \frac{f_a e_{i+1} y - f_m}{y} \tag{12}$$

as an expression for the upper bound of the TTE inherent in the ATN model (Eqs. 1–4). When calculating this model-inherent maximum TTE from the first to the second trophic level, the autotrophs' maximum biomass is their capacity K and not infinity, and Eq. 11 is used for the calculation instead of Eq. 12.

To differentiate the inherent TTE (upper bound of the TTE in the ATN model) from the actually obtained TTE during the dynamic simulations, the latter will thereafter be called obtained TTE.

Simulations

Biomasses and resulting values are mean values of the last 50,000 time steps of a 100,000 step time series. All calculations and figures were made using Python 2.7.6. For integration of the ordinary differential equations, the adaptive step-size lsoda solver was used with absolute and relative error tolerances $\varepsilon_{abs} = \varepsilon_{rel} = 10^{-13}$.

Table 2 Three trophic transfer efficiencies (TTE) are given, the maximum feasible TTE according to the given assimilation efficiencies (Table 1) and assuming that production equals respiration (Humphreys 1979) (Eq. 10), the maximum inherent TTE assuming maximum food concentration (Eq. 12), and the maximum TTE obtained from the simulations for both the original and the extended ATN versions for the three trophic levels in %

	Max. feasible TTE	Max. inherent TTE		Max. obtained TTE	
		Original	Extended	Original	Extended
$TTE_{3\to4}$	42.5	72.5	32.8	50.5	30.1
$TTE_{2\to3}$	42.5	72.5	32.8	44.5	30.2
$TTE_{1\to2}$	22.5	26.3	16.1	14.1	13.2

Results

We first evaluated the maximum inherent trophic transfer efficiency (TTE) assuming unlimited food supply. We found a value of 32.5% for the herbivores and 72.5% for the carnivores and top predators in the original ATN model, which exceeds by far the maximum feasible TTE of 22.5% for herbivores and 42.5% for carnivores and top predators (Eqs. 10, 12, Table 2). In the extended ATN version, the maximum inherent TTE was 16.1% for the herbivores and 32.8% for the carnivores and top predators (Eq. 12, Table 2). The maximum inherent TTE was smaller in the extended version as more carbon is respired instead of transported through the food chain to the upper trophic levels.

As a second and more practical step, we investigated the TTE obtained in dynamic simulations of a four trophic-level food chain using both the original and extended ATN versions over a gradient of the top predator's death rate constant d. In the extended ATN version, which accounts for activity and basal respiration separately, the maximum obtained TTE at trophic level 3 and 4 never exceeded the maximum feasible TTE (Fig. 2, Table 2, Eq. 10). In contrast, in the original ATN model the obtained TTE at trophic level 4 exceeded the maximum feasible TTE of 42.5% for $d > 0.0029$ (Fig. 2, maximum observed value 50.5%). At trophic level 3, the TTE of the carnivores in the original ATN model exceeded the maximum feasible TTE for small values of d ($d < 0.0006$, Fig. 2). The consistently lower obtained TTE in the extended ATN version indicates that this model version represents the energy transfer towards the higher trophic level more realistically than the original ATN model.

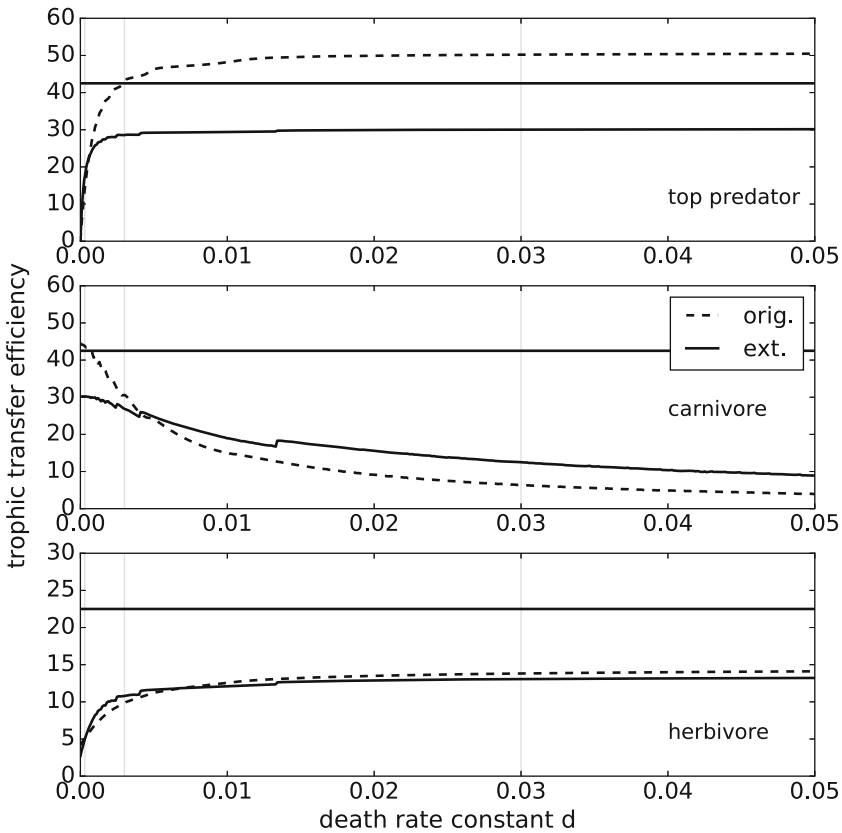

Fig. 2 Trophic transfer efficiency (TTE) obtained in simulations (in percent, defined as the production ratio of upper vs. lower trophic level) of the top predator (top panel), carnivore (center), and herbivore (bottom) in the original (dashed lines) and extended (solid lines) ATN versions for different top predator's death rate constants d. Gray vertical lines indicate the position of the biomass pyramids provided in Fig. 3. The horizontal lines indicate the maximum feasible TTE (see "Trophic transfer efficiency," Table 2)

With an increasing death rate constant d of the top predator, its own as well as the herbivore's obtained TTE increased, whereas the carnivore's obtained TTE decreased (Fig. 2). This alternating pattern of increasing and decreasing obtained TTE with increasing d resulted from a trophic cascade: Higher values of d lowered the top predator's biomass, which in turn lowered its total ingestion. Released from top-down control, the carnivore's biomass, and thus, its ingestion increased. This pattern propagated down to the herbivores and autotrophs. Since the TTE is a monotonously increasing function of the biomass on the respective lower trophic level (Eq. 11, Appendix, Fig. 7), this alternating pattern of decreasing and increasing biomasses translates directly to the TTEs on the different trophic levels.

The herbivore's obtained TTE remained below the maximum feasible TTE of 22.5% (Eq. 10) in both model versions (Fig. 2). The reason is the nonlinear dependence of the autotroph's production on its carrying capacity and its interaction with the nonlinear grazing function of the herbivore. When assuming a chain of three trophic levels where the carnivore as the highest trophic level experiences a quadratic death term, the herbivore was under strong top-down control and exceeded its maximum feasible TTE by up to a factor of 1.1 (Appendix, Figs. 5 and 6).

Depending on the top predator's death rate, the models exhibited different trophic cascade patterns. For small d (0.0003), the herbivore and the top predator accumulated high biomasses resulting in a top-heavy trophic cascade (Fig. 3a, d). For larger d (0.0030), the biomasses resembled roughly a column (Fig. 3b, e), and for higher d, a bottom-heavy trophic cascade occurred (Fig. 3c, f).

To further elucidate the reason for the inconsistencies between the obtained TTE of the original ATN model and physiological considerations and realistic estimates, we analyzed the carbon fluxes in the bottom-heavy trophic cascade (Fig. 3c, f) in more detail (Fig. 4, Table 3). The alternating biomasses indicate where the inconsistencies are most obvious. In the original ATN model, the top predator's respiration was small compared to its ingestion, resulting in a large production per ingested unit of carbon (Table 3). This led to a production being 33% higher than the respiration (Fig. 4b) and an obtained TTE of 50% (Fig. 4b, Table 3). In contrast, in the extended ATN version, the respiration per ingested unit of carbon was higher due to the activity respiration, which resulted in a lower production and an obtained TTE of 30% (Fig. 4a).

In the original ATN model, respiration per ingestion and production per ingestion varied considerably more between trophic levels than in the extended ATN version. This was due to the overemphasis of basal respiration and neglecting of the activity respiration: Only a high biomass (here, of the carnivore) resulted in respiration losses of substantially more than 50% of the assimilation and, thus, a realistic TTE in the original ATN model. In the extended ATN version, respiration per ingestion and production per ingestion did not vary that much across trophic levels even in the presence of a strong trophic cascade because respiration is not solely coupled to the standing biomass stock, but also to the assimilation. As low biomasses are connected with high per capita rates in the ATN models, a low biomass-related basal respiration is counteracted by high activity respiration and vice versa.

Discussion

Allometric trophic network (ATN) models are an important tool to analyze dynamics of food webs (Boit et al. 2012; Hudson and Reuman 2013; Schuwirth and Reichert 2013; Kuparinen et al. 2016) and their diversity and stability (Brose et al. 2006; Rall et al. 2008; Berlow et al. 2009; Heckmann et al. 2012). Despite their frequent use, the ATN energetics was not yet explicitly addressed, though it decisively influences dynamic patterns of the model (Boit et al. 2012). Here, we compared the energetics of the original ATN model (Yodzis and Innes 1992; Brose et al. 2006) which considers only basal respiration, and an extended ATN version (Boit et al. 2012) including both basal and activity respiration. We found that the trophic transfer efficiency (TTE) could become unrealistically high in the original ATN model in both static calculations and dynamic simulations, whereas it always fell into a physiologically and ecologically realistic range in the extended ATN version. The reason for the more realistic energy transfer is the inclusion of the activity respiration that depends on the amount of assimilated carbon in the extended ATN version.

The threshold above which we consider a TTE unrealistically high was set very conservatively and followed from the assumption that the energy allocated to production can at most be equal to respiration (Humphreys 1979). This yields a maximum feasible TTE of 22.5% for herbivores and 42.5% for carnivores (Eq. 10). These upper theoretical limits are usually not reached in natural communities even when dominated by unicellular organisms or invertebrates, except when a trophic level is under high predation pressure. Empirically established maximum TTE ranges between 13% and around 30% for both herbivores and carnivores from pelagic systems and including small to large fish (Straile 1997; Jennings et al. 2002; Barnes et al. 2010). The extended ATN version reflects these natural energetic constraints well by keeping the obtained TTE in a realistic range up to 30% (cf. Fig. 2). In contrast, the original ATN model led to an obtained TTE up to 51% (cf. Fig. 2) which overestimates the empirical values of at most 30% by a factor of 1.7.

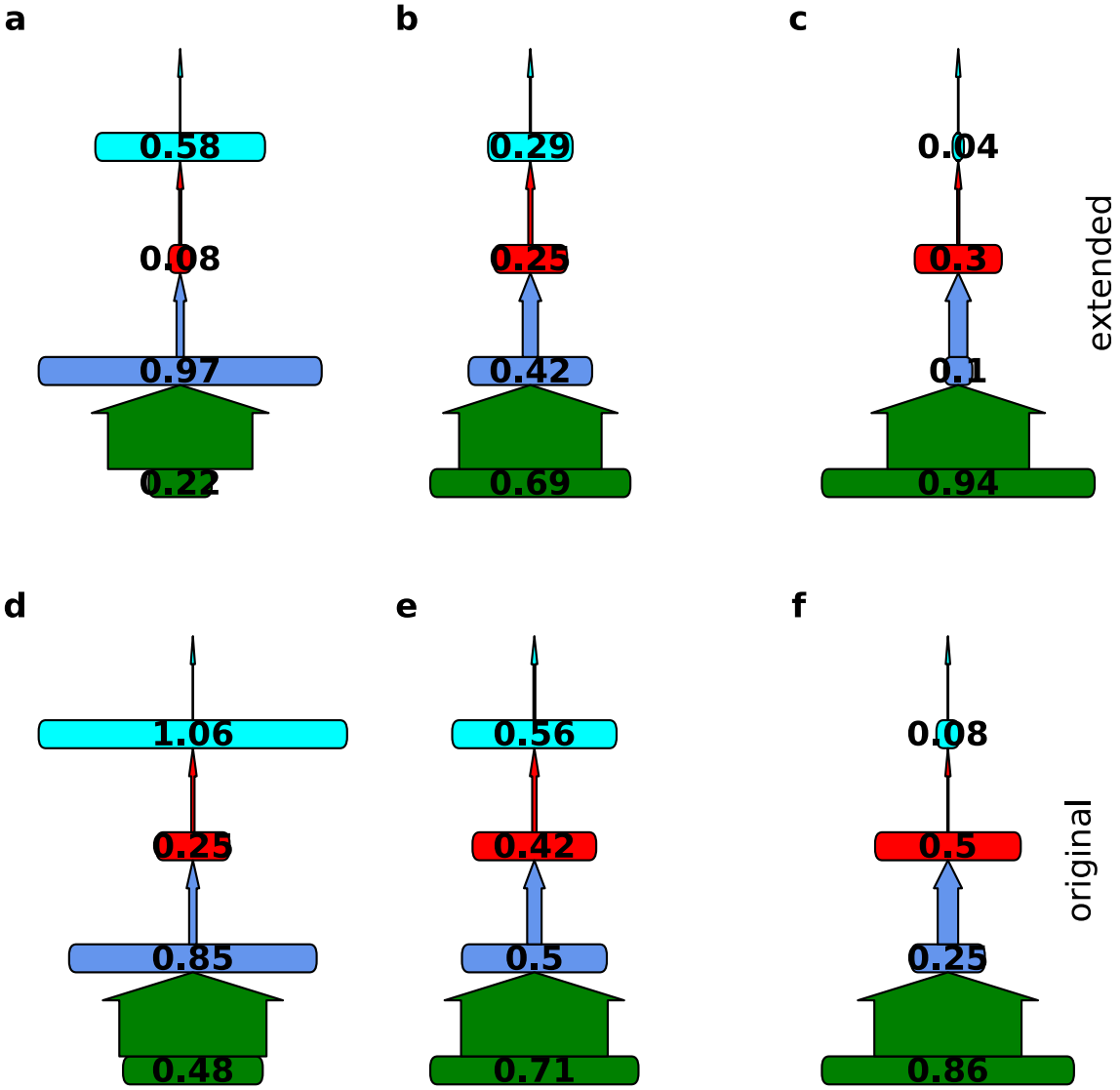

Fig. 3 Comparison of the mean biomasses (bold numbers) within the food chain of the extended ATN version including activity respiration (**a**–**c**) and the original ATN model (**d**–**f**), for different top predator's death rate constants $d = 0.0003$ (**a**, **d**), $d = 0.003$ (**b**, **e**), and $d = 0.03$ (**c**, **f**). Arrows indicate production rates. Their width is scaled to autotroph's production as 100%. Box widths are scaled with the species' biomasses

The metabolic theory of ecology does not differentiate between basal respiration proportional to the standing biomass stock and activity respiration (Brown et al. 2004). Brown et al. (2004) stated that the metabolic rate generally depends only on biomass and that the field metabolic rate, analog to our activity respiration, is a "fairly constant multiple of the basal rate" and therefore also depends only on the biomass. A similar assumption also served as basis for the ATN models accounting only for basal respiration proportional to the biomass. This assumption is reasonable if resource levels are fairly constant; however, biomasses and ingestion rates vary in nature and dynamic models and so does, ultimately, also the TTE (Appendix, Fig. 7).

The different patterns of trophic cascades illustrate the problematic consequences of linking respiration only to biomass. The amount of top-down control exerted by the top predator or the carnivore, and thus the strength of the trophic cascade were modulated by the death rate constant d. For small d, the top predator had a high biomass and controlled the carnivore. The carnivore's obtained TTE then became unrealistically high in the original ATN model, and the food web became (too) top heavy. The link between a high TTE and top heavy food webs is also described in a review of 23 food webs (McCauley et al. 2018). For intermediate d, the biomasses were approximately equally distributed across different trophic levels which is in line with the flat biomass distribution established for pelagic systems (Gaedke 1992). For higher d, the top predator was top-down controlled by its death rate and released the carnivore from grazing pressure, but

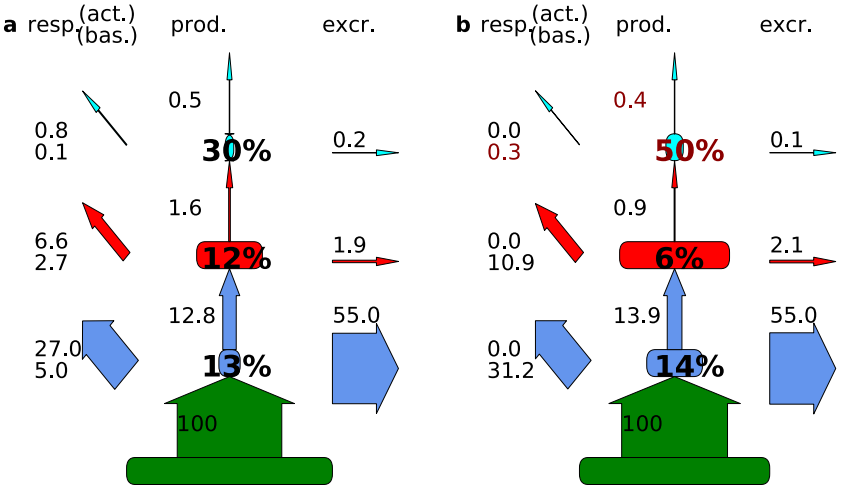

Fig. 4 Comparison of the energy transfer within the food chain of the extended ATN version including activity respiration (**a**), and the original ATN model (**b**). The biomass pyramids are based on the same data as Fig. 3c, f, i.e., $d = 0.03$. Included values are basal and activity respiration (numbers on the left, activity above basal respiration), production (numbers in the middle to the left of the upward arrows), trophic transfer efficiency (bold large numbers), and excretion (numbers above the right arrows). All fluxes are standardized to autotroph's production as 100%, so that wider arrows indicate larger values. Box widths are scaled with the species' biomasses. Red values point out inconsistencies with the physiological considerations that respiration is equal to or less than production (Humphreys 1979)

in this case, the top predator's obtained TTE became unrealistically high. In any case, the obtained TTE was too high at one particular trophic level within a pronounced trophic cascade because the top-down controlled trophic levels had a low biomass and thus a low basal respiration. Thus, the assumption of Brown et al. (2004) that activity respiration and field metabolic rate are proportional to a standing biomass stock only holds for equally distributed biomasses, but not for unequally distributed biomasses in trophic cascades.

The link between activity respiration and ingestion as we introduced it here to the ATN model allows for a more flexible reaction to dynamic instead of constant biomasses. This is important when modeling large food webs with rapidly changing dynamics such as pelagic systems. ATN and other food web models are known to form trophic cascades (Carpenter et al. 2016) which are observed in many ecosystems (Carpenter et al. 1985; Pace et al. 1999; Shurin et al. 2002) and, as we showed here, strongly affects the TTE. Other ATN models dampened the trophic cascades with mechanism such as predator interference or type III functional response which obfuscates this underlying energetic problem to some extent (Rall et al. 2008). However, they do not solve it, as the model-inherent TTE is independent of these mechanisms. The ATN approach has also been used to parameterize large-scale ecosystem models such as the Madingley model (Harfoot et al. 2014). In this model, neglecting activity respiration seems to have contributed to unrealistically top heavy biomass distributions as well, underlining the importance of more accurate assumptions regarding basic energetic processes than the original ATN provides. The pronounced trophic cascades as seen in our study are due to the structurally simplistic food chain and would be dampened in natural systems, e.g., by a higher trophic connectance via omnivory.

Other models, like Rosenzweig-MacArthur-type predator-prey models (Rosenzweig and MacArthur 1963; Weitz and Levin 2006), incorporate respiration losses only by a constant factor named conversion efficiency related to ingestion and production; thus, this type of model only accounts for (what we call here) activity respiration. Basal respiration may be implicitly considered in a death rate proportional to the biomass. Anderson (1992) pointed out the difference between basal and activity respiration

Table 3 Respiration to ingestion ratio (R/I) and production to ingestion ratio (P/I ≙ obtained TTE since non-grazing mortality was not included in the ATN model for the 1st–3rd trophic level; thus, the production of the trophic level below is ingested entirely, see "ATN model equations") for both the original (orig.) and extended (ext.) ATN versions with the top predator's death rate constant $d = 0.03$. Autotrophic respiration is already included in the growth rate and therefore not listed here. Values were calculated from the biomass, respiration, and production values shown in Figs. 3f and 4b for the original ATN model, and in Figs. 3c and 4a for the extended ATN version, respectively

	R/I		P/I ≙ TTE	
	orig. (%)	ext. (%)	orig. (%)	ext. (%)
Top predator	35	55	50	30
Carnivore	79	72	6	12
Herbivore	31	32	14	13

especially for unicellular organisms and invertebrates whose activity respiration exceeds the basal respiration as they are poikilotherms with low maintenance costs when inactive. In our extended ATN version, we combined both respiration rates and implemented these ideas by introducing the factor f_a in the formulation of assimilation (cf. Eq. 8, "Methods," Fig. 1), thereby making activity respiration proportional to the amount of assimilated carbon.

Following Boit et al. (2012), we set the parameter $f_a = 0.4$ for all consumers assuming that respiration is slightly larger than production (Humphreys 1979). Although this conservative estimate satisfies fundamental energetic constraints, a more differentiated picture may emerge when defining a more empirically grounded value range for f_a for different taxa. In the same way, the parameter $f_m = 0.1$ (following Boit et al. (2012)) may be adapted to fit different taxa. As a recent meta-analysis reveals that the differences in respiration rates between taxonomic groups are not only due to consumer type (e.g., herbivore or carnivore) (Lang et al. 2017), future research could aim to entangle the influences of taxonomic group, activity, and food availability on respiration rates. Until then, due to the scarcity of experimental data on activity vs. basal respiration rates of invertebrates, the parameterization of f_a and f_m in a specific food web context remains a challenge for future modeling studies with ATNs.

The complexity of the model did not increase from a mathematical point of view even though we introduced two additional parameters (f_a and f_m) in the extended ATN version. The number of effective parameters that independently determine model dynamics is the same in the original and the extended ATN versions. This becomes obvious when we introduce new parameters for the extended ATN model: $e_{\mathrm{prod},i} = e_i f_a$ as the production efficiency (equivalent to e_i in the original model) and $x_{b,i} = f_m x_i$ (equivalent to x_i in the original model) as the per capita basal metabolic rate. When aiming for a concise mathematical description of the model, we recommend to use these effective parameters. Here, however, we chose not to do so in order to emphasize the underlying biological processes. In the same vein, we argue that we do not merely propose to use different values for some parameters of the ATN model, but stress the conceptual advancement of the ATN model by clearly distinguishing between basal and activity respiration, which is essential for improving quantitative predictions about ecosystem energetics.

To conclude, basal and activity respiration depend on different processes and should both be considered explicitly in models covering metabolic processes. Including activity respiration in the ATN model lowers the obtained TTE to realistic values in comparison to empirically derived values. Especially for food webs mainly based on unicellular organisms and invertebrates or modeling ecosystems prone to trophic cascading, we recommend using the extended ATN version to achieve more realistic energetics. Far more than a mere modeling fix, reflecting the energy flux through food webs in a realistic way is indispensable for upscaling and integrating smaller modules to larger community networks or even large-scale ecosystem models. ATN models will then be ready for quantitatively linking trophic interactions in biodiverse communities to ecosystem-level biomass dynamics and biogeochemical cycling.

Acknowledgments We thank P. de Ruiter and two anonymous reviewers for helpful comments on an earlier version of the manuscript.

Funding information This work was funded by DFG (GA 401/26-1) as part of the Priority Programme 1704 (DynaTrait).

Appendix

We also modeled a three trophic-level food chain in which the carnivore has a density-dependent death rate equivalent to the top predator in the chain of four trophic levels (Eq. 4). With this model setup, we examined the herbivore's obtained TTE when being released from top-down control due to increasing the carnivore's death rate.

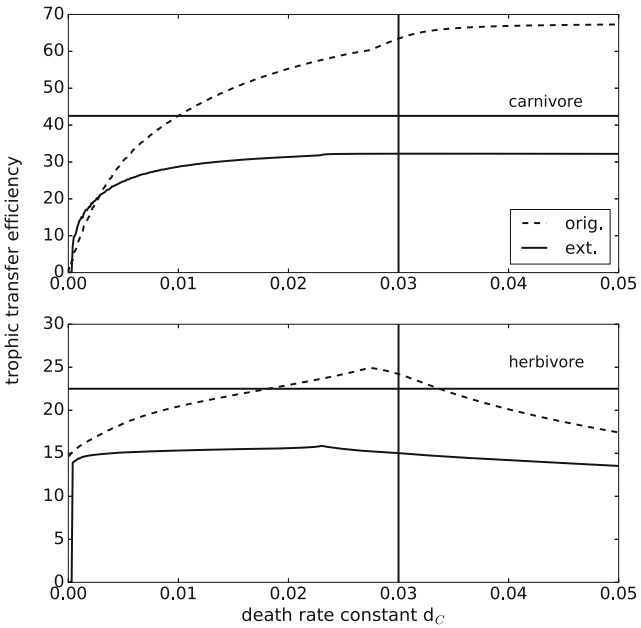

Fig. 5 Trophic transfer efficiency (obtained TTE, defined as the production ratio of upper vs. lower trophic level) of the carnivore (upper panel) and herbivore (bottom) in the original (dashed lines) and extended (solid lines) ATN versions for different carnivore's death rate constants d. For one parameter value (vertical line), the biomass pyramids are provided in Fig. 6. The horizontal lines indicate the maximum feasible TTE (Eq. 10, Table 2)

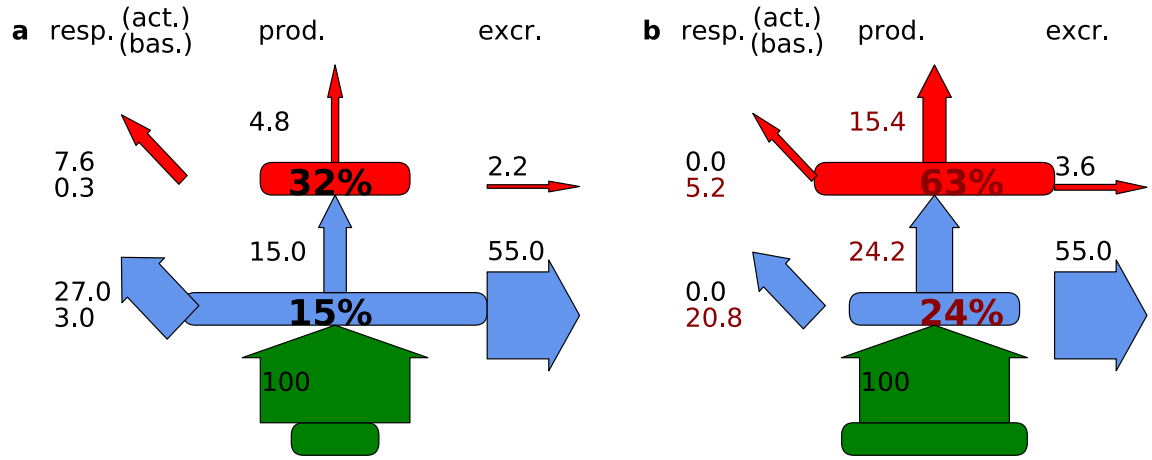

Fig. 6 Comparison of the energy transfer within a three trophic-level food chain of the extended ATN version including activity respiration (**a**) and the original ATN model (**b**). The biomass pyramids are based on the parameter indicated in Fig. 5, i.e., $d = 0.03$. Included values are basal and activity respiration (numbers on the left, activity above basal respiration), production (numbers in the middle to the left of the upward arrows), trophic transfer efficiency (bold large numbers), and excretion (numbers above the right arrows). All fluxes are standardized to autotroph's production as 100%, so that wider arrows indicate larger values. Box widths are scaled with the species' biomasses. Red values point out inconsistencies with the physiological considerations that respiration is equal to or less than production (Humphreys 1979)

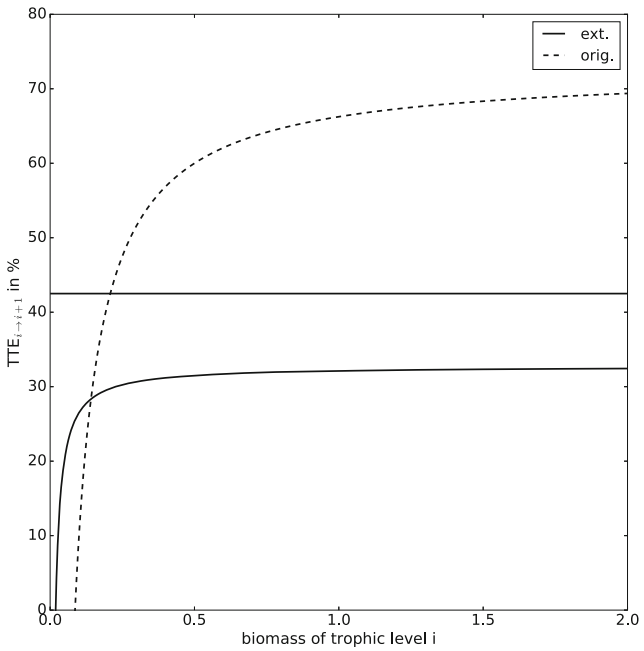

Fig. 7 Trophic transfer efficiency (obtained TTE in %, defined as the production ratio of upper vs. lower trophic level) of a trophic level $i + 1$ (here, parameterized for both the carnivore and the top predator as they have the same assimilation efficiency) in the original (dashed line) and extended (solid line) ATN versions for different food quantities (biomass of the lower trophic level i). The horizontal line indicates the maximum feasible TTE (Eq. 10, Table 2)

References

Anderson TR (1992) Modelling the influence of food C:N ratio, and respiration on growth and nitrogen excretion in marine zooplankton and bacteria. J Plankton Res 14:1645–1671. https://doi.org/10.1093/plankt/14.12.1645

Barnes C, Maxwell D, Reuman DC, Jennings S (2010) Global patterns in predator-prey size relationships reveal size dependency of trophic transfer efficiency. Ecology 91:222–232. https://doi.org/10.1890/08-2061.1

Begon M, Townsend CR, Harper JL (2006) Ecology—from individuals to ecosystems, 4th edn. Blackwell Publishing Malden, Mass

Benoît E, Rochet M-J (2004) A continuous model of biomass size spectra governed by predation and the effects of fishing on them. J Theor Biol 226:9–21. https://doi.org/10.1016/S0022-5193(03)00290-X

Berlow EL, Dunne JA, Martinez ND, Stark PB, Williams RJ, Brose U (2009) Simple prediction of interaction strengths in complex food webs. Proc Natl Acad Sci 106:187–191. https://doi.org/10.1073/pnas.0806823106

Boit A, Martinez ND, Williams RJ, Gaedke U (2012) Mechanistic theory and modelling of complex food-web dynamics in Lake Constance. Ecol Lett 15:594–602. https://doi.org/10.1111/j.1461-0248.2012.01777.x

Brose U (2008) Complex food webs prevent competitive exclusion among producer species. Proc Biol Sci 275:2507–2514. https://doi.org/10.1098/rspb.2008.0718

Brose U, Williams RJ, Martinez ND (2006) Allometric scaling enhances stability in complex food webs. Ecol Lett 9:1228–1236. https://doi.org/10.1111/j.1461-0248.2006.00978.x

Brown JH, Gillooly JF, Allen AP, Savage VM, West GB (2004) Toward a metabolic theory of ecology. Ecology 85:1771–1789. https://doi.org/10.1890/03-9000

Carpenter SR, Kitchell JF, Hodgson JR (1985) Cascading trophic interactions and lake productivity. Bioscience 35:634–639. https://doi.org/10.1525/bio.2010.60.10.17

Carpenter SR, Cole JJ, Pace ML, Wilkinson GM (2016) Response of plankton to nutrients, planktivory and terrestrial organic matter: a

model analysis of whole-lake experiments. Ecol Lett 19:230–239. https://doi.org/10.1111/ele.12558

Gaedke U (1992) The size distribution of plankton biomass in a large lake and its seasonal variability. Limnol Oceanogr 37:1202–1220

Gaedke U, Hochstädter S, Straile D (2002) Interplay between energy limitation and nutritional deficiency: empirical data and food web models. Ecol Monogr 72:251–270. https://doi.org/10.1890/0012-9615(2002)072[0251:IBELAN]2.0.CO;2

Gessaman JA (1973) Methods of estimating the energy cost of free existence. In: Logan UT (ed) Ecological energetics of homeotherms. Utah State University Press, Logan, Utah, pp 3–31

Harfoot MBJ, Newbold T, Tittensor DP, Emmott S, Hutton J, Lyutsarev V, Smith MJ, Scharlemann JPW, Purves DW (2014) Emergent global patterns of ecosystem structure and function from a mechanistic general ecosystem model. PLoS Biol 12:e1001841. https://doi.org/10.1371/journal.pbio.1001841

Heckmann L, Drossel B, Brose U, Guill C (2012) Interactive effects of body-size structure and adaptive foraging on food-web stability. Ecol Lett 15:243–250. https://doi.org/10.1111/j.1461-0248.2011.01733.x

Hendriks AJ (1999) Allometric scaling of rate, age and density parameters in ecological models. Oikos 86:293–310. https://doi.org/10.2307/3546447

Holling CS (1959) Some characteristics of simple types of predation and parasitism. Can Entomol 91:385–398

Hudson LN, Reuman DC (2013) A cure for the plague of parameters: constraining models of complex population dynamics with allometries. Proc R Soc B Biol Sci 280:20131901. https://doi.org/10.1098/rspb.2013.1901

Humphreys WF (1979) Production and respiration in animal populations. J Anim Ecol 48:427–453. https://doi.org/10.2307/4171

Jennings S, Warr KJ, Mackinson S (2002) Use of size-based production and stable isotope analyses to predict trophic transfer efficiencies and predator-prey body mass ratios in food webs. Mar Ecol Prog Ser 240:11–20. https://doi.org/10.3354/meps240011

Kuparinen A, Boit A, Valdovinos FS, Lassaux H, Martinez ND (2016) Fishing-induced life-history changes degrade and destabilize harvested ecosystems. Sci Rep 6:1–9. https://doi.org/10.1038/srep22245

Lang B, Ehnes RB, Brose U, Rall BC (2017) Temperature and consumer type dependencies of energy flows in natural communities. Oikos 4:1–9. https://doi.org/10.1111/oik.04419

McCauley DJ, Gellner G, Martinez ND et al (2018) On the prevalence and dynamics of inverted trophic pyramids and otherwise top-heavy communities. Ecol Lett 21:439–454. https://doi.org/10.1111/ele.12900

Pace ML, Cole JJ, Carpenter SR, Kitchell JF (1999) Trophic cascades revealed in diverse ecosystems. Trends Ecol Evol 14:483–488. https://doi.org/10.1016/S0169-5347(99)01723-1

Rall B, Guill C, Brose U (2008) Food-web connectance and predator interference dampen the paradox of enrichment. Oikos 117:202–213. https://doi.org/10.1111/j.2007.0030-1299.15491.x

Rosenzweig MI, MacArthur RH (1963) Graphical representation and stability conditions of predator-prey interactions. Am Nat 97:209–223. https://doi.org/10.1086/662677

Schneider FD, Scheu S, Brose U (2012) Body mass constraints on feeding rates determine the consequences of predator loss. Ecol Lett 15:436–443. https://doi.org/10.1111/j.1461-0248.2012.01750.x

Schneider FD, Brose U, Rall BC, Guill C (2016) Animal diversity and ecosystem functioning in dynamic food webs. Nat Commun 7:12718. https://doi.org/10.1038/ncomms12718

Schuwirth N, Reichert P (2013) Bridging the gap between theoretical ecology and real ecosystems: modeling invertebrate community composition in streams. Ecology 94:368–379. https://doi.org/10.1890/12-0591.1

Shurin JB, Borer ET, Seabloom EW, Anderson K, Blanchette CA, Broitman B, Cooper SD, Halpern BS (2002) A cross-ecosystem comparison of the strength of trophic cascades. Ecol Lett 5:785–791. https://doi.org/10.1046/j.1461-0248.2002.00381.x

Straile D (1997) Gross growth efficiencies of protozoan and metazoan zooplankton and their dependence on food concentration, predator-prey weight ratio, and taxonomic group. Limnol Oceanogr 42:1375–1385. https://doi.org/10.4319/lo.1997.42.6.1375

Weitz JS, Levin SA (2006) Size and scaling of predator-prey dynamics. Ecol Lett 9:548–557. https://doi.org/10.1111/j.1461-0248.2006.00900.x

Yodzis P, Innes S (1992) Body size and consumer-resource dynamics. Am Nat 139:1151–1175. https://doi.org/10.1086/285380